Inorganic Chemistry

ARTICLE

pubs.acs.org/IC

Control of On−Off or Off−On Fluorescent and Optical [Cu^{2+}] and [Hg^{2+}] Responses via Formal Me/H Substitution in Fully Characterized Thienyl "Scorpionate"-like BODIPY Systems

Kibong Kim,[†,‡] Shin Hei Choi,[†,‡] June Jeon,[†,‡] Hyosun Lee,[§] Jung Oh Huh,[‡] Jaeduk Yoo,[∥] Jong Taek Kim,[‡] Chang-Hee Lee,[∥] Yoon Sup Lee,[‡] and David G. Churchill*[,†,‡]

[†]Molecular Logic Gate Laboratory and [‡]Department of Chemistry and School of Molecular Science, Korea Advanced Institute of Science and Technology (KAIST), 373-1 Guseong-dong, Yuseong-gu, Daejeon, 305-701, Republic of Korea

[§]Organometallic Chemistry Laboratory, Department of Chemistry (BK 21), Kyungpook National University, Daegu 702-701, Republic of Korea

[∥]Department of Chemistry, Kangwon National University, Chun-Chon 200-701, Republic of Korea

Supporting Information

ABSTRACT: One 8-phenyl and two 8-mesityl-substituted "scorpionate"-like BODIPY-type species of the formula [3,4,4-tris(5-*R*-(2-thienyl))-8-(2,4,6-*R*′-phenyl)-4-bora-3a,4a-diaza-*s*-indacene (R = H, R′ = H, **3a**; R, = H, R′ = Me, **2a**; R, = Me, R′ = Me, **2b**)] have been synthesized and fully characterized. Importantly, differences in their solution (MeCN) optical Cu^{2+} and Hg^{2+} probing capacity via *SSS*-chelation were investigated. Compounds **2a**−**3a** were prepared from the requisite 8-substituted BODIPY complexes. They were characterized first by complete ^{1}H, ^{11}B and ^{13}C NMR spectroscopic assignments (CD_3Cl or $CD_3C(O)CD_3$); the molecular structures of **2a** and **3a** were determined by X-ray crystallography. Compounds **2a**−**3a** were studied by UV−vis and fluorescence spectroscopy [Φ_F = 0.27 ± 0.013 (**2a**); 0.024 ± 0.0016 (**2b**); 0.0034 ± 0.00047 (**3a**)]. Importantly, low [Cu^{2+}] with **3a** (<3.0 × 10^{-5} M) gave rise to an increase of fluorescence intensity (off−on; 6.3-fold), whereas with **2a** it decreased (on−off). When [Hg^{2+}] (<3.0 × 10^{-5} M) was added to **2b**, the $\lambda_{em,max}$ value increased (off−on; 3.2-fold), and for **2a**, it decreased (on−off). The association constant (K_a) for Hg^{2+}·**2a** was determined to be 3120 ± 307 M^{-1}. An approximate stoichiometric 1:1 binding determined by Job plot analysis is in line with successful DFT modeling of *SSS*-Cu^{2+} binding for this system type. ^{1}H NMR spectroscopy also revealed tentative sets of product complex peaks. These simple differences caused by formal ligand Me-group incorporation are the first for any related fluorophores, to the best of our knowledge.

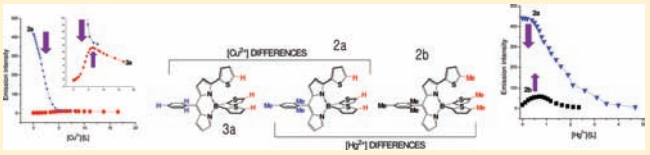

INTRODUCTION

Selective molecular sensing of metal ions continues to be a practical research aim in both biological and environmental chemistry. Deviations from proper metal ion regulation (normal concentration ranges of, e.g., Cu^{2+}, Zn^{2+}, and Fe^{n+}) in biological systems may lead to, or signal, disease. Heavy metals such as Hg^{2+} and Pb^{2+} are also important sensing targets because, while they occur naturally, certain species continue to persist in the environment as contaminants that stem from anthropogenic root causes; they are of grave concern if they are present in the body at high concentrations. Cupric ion sensing has been a recent research aim for chemists and other researchers and is considered important because of the correlations Cu^{2+} concentrations have with distinct changes in biological systems (especially neurological systems) and in resulting pathology. In particular, Cu^{2+} concentration is thought to be an important standard, or causative agent, in protein misfolding and in several neurodegenerative diseases.[1−4] While achieving such detection adequately is marked by challenges (Cu^{2+} being a "universal" fluorescence quencher), recent and leading references for optical Cu^{2+} sensing/detection[5−8] underscore the degree to which synthetic chemistry holds a command over future synthetic receptor designs, so to offer more options in off−on optical signaling.

Clearly, many challenges still remain in achieving optimal selectivity and "turn-on" behavior. Separately, Hg^{2+} sensing is interesting in environmental chemistry.[9−11] Molecular and ionic recognition involving "turn-on" fluorescence intensity with Hg^{2+} is also challenging because of its quenching nature.

Fluorescence is a sensitive technique. It often relates to various soluble organic-based molecules that are planar, rigid, and π-delocalized and is even scalable to where the emissions of single molecules can be detected. BODIPY-type systems (Figure 1) are common fluorophore derivatives that continue to be explored actively.[12,13] Thus, further development can be thought of in terms of imparting by derivatization a variety of features (photophysical, solubility, functional groups) advantageous in biotechnology

Received: August 18, 2010
Published: May 20, 2011

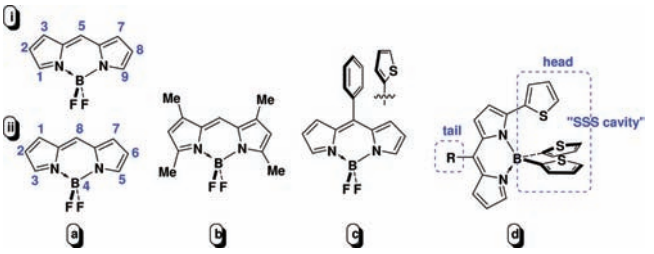

Figure 1. Some common types of BODIPY derivatives: (a) plain BODIPY[30] with (i) dipyrrin numbering and (ii) indacene numbering (numbering used in the text); (b) difluoroboryl-1,3,5,7-tetramethyldipyrrin; (c) difluoroboryl(8-phenyl)- or -8-(2-thienyl)dipyrrin; (d) "scorpionate-like" BODIPY-type species.

(e.g., bioprobing). BODIPY-type systems have previously addressed copper cation[14−20] and Hg^{2+} detection.[21−29]

The "scorpionate-like" design involves the BODIPY fluorogenic core in which there has been substitution of the fluoride groups by aryl groups (Figure 1d). The substitution of aryl groups in place of the two 4-boron position fluorides was first reported by Ziessel et al., and these groups extend to phenyls, thiophenes, and larger aromatic systems.[12,18,31] We have been involved with the synthesis and characterization of 2- and 3-thienyl-containing di- and polypyrrolic species in trying to uncover versatile and robust low molecular weight (MW) multifunctional probe precursors, preferably related to molecular neurodegeneration applications. We have previously prepared a system that exhibited discrete sensing responses to Cu^{2+} and Hg^{2+} in solution.[18] Our recent reports with BODIPY-based chromophores, in terms of M^{n+} sensing, have involved a novel SSS "scorpionate-like" binding cavity (Figure 1d). These reports raise the question of whether the $[N_2BAr_2]$ unit is satisfactory because it results in a derivative with a lowered fluorescence quantum yield (Φ_F).[32]

Our original interest in simple 8-substituted species derives from a report by Holten and co-workers,[32] in which it was found that the simple formal replacement of [H] with one methyl substituent at the "tail" phenyl (*o*-tolyl) gives a dramatic increase in Φ_F. A related report comes from Sun et al., who reported a BODIPY species in which the 8-position was a 2-hydroxy-5-methoxyphenyl group. This group undergoes selective oxidation with hypochlorous acid to afford a 2,5-quinonyl moiety, whereupon a "turn-on" green fluorescence response is observed from the molecule.[33] Also, BODIPY species in which oxidation of a thienyl substituent at the 8-position has also been reported.[31] In terms of thienyl derivatization, there are now new ways to functionalize the BODIPY core with such heterocycles. Namely, facile and high-yielding access to the thienyl 8-substitution is available via coupling chemistry at the 8-position of the 8-substituted [−SMe] derivative, as reported recently by Peña-Cabrera and co-workers.[34] In the present report, we consider the BODIPY receptor "head" position bearing thienyl motifs and the [SSS] core with a phenyl-based *meso* 8-position "tail" removing possible ambiguity resulting from M^{n+} binding capability of the "tail" *S*-donor atom which was present in earlier systems.[18,31,35] The substitution pattern in the present system allows for the quantification of the $[CH_3]$ substitution effect, in terms of metal ion [on−off] and [off−on] sensing behavior differences. Herein, we discuss the synthesis, detailed multinuclear NMR characterization, optical properties, and structural aspects of three new "scorpionate"-like BODIPY species that are 8-mesityl/phenyl-substituted [3,4,4-tris(5-R-(2-thienyl))-8-(2,4,6-R′-phenyl)-4-bora-3a,4a-diaza-*s*-indacene (R, R′= H, **3a**; R = H, R′ = Me, **2a**; R = R′ = Me, **2b**)]. This was studied in the context of exploring new small molecule possibilities in metal ion recognition.

2. EXPERIMENTAL METHODS

General Considerations. All solvents and chemicals used in the following synthetic steps were of analytical grade and used as received from reliable commercial sources. The reagents 2-thienyllithium, THF, 2-methylthiophene, and *n*-butyllithium in THF solution were purchased from Aldrich Chemical Co.; methanol was purchased from Merck Chemical Co. Compounds **2** and **3** have been reported previously.[32] The synthetic details for the preparation of **2** and **3** were followed herein. Compound **1** was prepared by us but is also accessible via the facile coupling route reported by Peña-Cabrera et al.[34] All solvents used for NMR spectral analysis were purchased commercially and were of spectroscopic grade. UV−vis absorption and emission spectra are obtained using a CARY 300 Bio UV−vis spectrometer and a Shimadzu RF-5301 PC spectrophotometer, respectively. Emission spectra were acquired through the excitation at the $\lambda_{abs,max}$ value, as assigned in the UV−vis absorption spectra for each compound. Fluorescein in 0.1 N NaOH (Φ_F = 0.92)[36] was used as the standard for the fluorescence quantum yield (Φ_F) measurements. C, H, and N elemental analyses were measured for **2a**, **2b**, and **3a** using a Vario EL III CHNS elemental analyzer. High-resolution MALDI mass spectrometry was performed on a Bruker Autoflex III with a Nd YAG laser source (355 nm) by the research support staff at KAIST (Daejeon, South Korea) for **2a**, **2b**, and **3a**. HRMS was performed with a Bruker micrOTOF II mass spectrometer. ^{1}H, ^{13}C, and ^{11}B NMR spectra were obtained on a Bruker Avance 300 or 400 MHz spectrometer. Spectral signals were calibrated by the protio impurity of the deuterated solvent. Tetramethylsilane ($Si(CH_3)_4$) was used as an internal NMR spectral standard.

Synthesis of Compound ***2a*** *[3,4,4-Tri(2-thienyl)-8-(2,4,6-trimethylphenyl)-4-bora-3a,4a-diaza-s-indacene].* Compound **2** was prepared by us through a literature method.[37] Compound **2** (0.30 g, 0.97 mmol) was dissolved in anhydrous THF (20 mL) and stirred at −78 °C for 10 min. Into this solution, a sample of 2-thienyllithium was slowly added (2.6 mL, 1.0 M in THF). Generally, the synthetic procedure for compound **2a** was similar to that for **1a**.[18] Finally, compound **2a** was isolated via recrystallization in methanol (0.20 g, 39%). ^{1}H NMR spectral signals ($CD_3C(O)CD_3$: δ 2.05, 400 MHz): δ 7.57 (t, $^3J_{H-H}$ = 1.5, 1H$_h$), 7.40 (dd, $^3J_{H-H}$ = 5.1 Hz, $^3J_{H-H}$ = 3.8 Hz, 1H$_j$), 7.31 (dd, $^3J_{H-H}$ = 3.8 Hz, $^3J_{H-H}$ = 1.0 Hz, 2H$_m$), 7.12 (dd, $^3J_{H-H}$ = 3.4 Hz, $^4J_{H-H}$ = 1.0 Hz, 2H$_l$), 7.06 (s, 2H$_b$), 6.95 (dd, $^3J_{H-H}$ = 4.8 Hz, $^4J_{H-H}$ = 1.5 Hz, 2H$_n$), 6.93 (dd, $^3J_{H-H}$ = 3.5 Hz, $^4J_{H-H}$ = 1.1 Hz, 1H$_k$), 6.86 (d, $^3J_{H-H}$ = 4.4 Hz, 1H$_e$), 6.83 (d, $^3J_{H-H}$ = 4.4 Hz, 1H$_d$), 6.76 (dd, $^3J_{H-H}$ = 5.1 Hz, $^4J_{H-H}$ = 1.1 Hz, 1H$_i$), 6.56 (dd, $^3J_{H-H}$ = 4.26 Hz, $^4J_{H-H}$ = 1.2 Hz, 1H$_f$), 6.44 (dd, $^3J_{H-H}$ = 4.26 Hz, $^3J_{H-H}$ = 1.85 Hz, 1H$_g$), 2.37 (s, 3H$_{c'}$), 2.14 (s, 6H$_{a'}$). ^{13}C NMR spectral signals ($CD_3C(O)CD_3$: δ 30.0, 100 MHz): δ 152.8 (m, 1C$_S$), 145.4 (s, 1C$_2$), 145.1 (dt, $^1J_{C-H}$ = 183.7 Hz, $^2J_{C-H}$ = 9.0 Hz, 1C$_h$), 139.4 (m [*looks like: q,* $^2J_{C-H}$ = *6.0 Hz*], 1C$_c$), 137.7 (m, [*looks like: t,* $^2J_{C-H}$ = *8.7 Hz*] 1C$_3$), 137.1 (m, 2C$_a$), 134.9 (m, 1C$_6$), 133.9 (m [*looks like: q,* $^2J_{C-H}$ = *8.6 Hz*], 1C$_4$), 132.5 (dm, $^1J_{C-H}$ = 155.2 Hz, 1C$_k$), 131.6 (m, 1C$_1$), 131.0 (dm, $^1J_{C-H}$ = 146.2 Hz, 2C$_l$), 129.9 (dm, $^1J_{C-H}$ = 203.7 Hz, 1C$_j$), 129.8 (dm, $^1J_{C-H}$ = 170.8 Hz, 1C$_d$), 129.0 (dm, $^1J_{C-H}$ = 130.6 Hz, 2C$_b$), 128.1 (dm, $^1J_{C-H}$ = 161.9 Hz, 1C$_i$), 128.0 (dm, $^1J_{C-H}$ = 172.7 Hz, 2C$_n$), 127.4 (dm, $^1J_{C-H}$ = 164.6 Hz, 2C$_m$), 127.2 (dm, $^1J_{C-H}$ = 175.0 Hz, 1C$_f$), 122.7 (dd, $^1J_{C-H}$ = 174.1 Hz, $^2J_{C-H}$ = 3.9 Hz, 1C$_e$), 119.2 (ddd, $^1J_{C-H}$ = 174.1 Hz, $^2J_{C-H}$ = 8.6 Hz, $^2J_{C-H}$ = 3.1 Hz, 1C$_g$), 21.2 (q, $^1J_{C-H}$ = 125.9 Hz, $^3J_{C-H}$ = 5.3 Hz, 1C$_{c'}$), 20.0 (q, $^1J_{C-H}$ = 125.9 Hz, $^3J_{C-H}$ = 4.9 Hz, 2C$_{a'}$). ^{11}B NMR spectral signals (CD_3COCD_3, BF_3OEt_2:

δ 0.00, 128 MHz): δ −2.00 (s), MALDI-TOF *m/z* (M^+): 520.13 (calcd) 520.64 (obsd). HRMS *m/z* ($(M + Na)^+$): 543.117 (calcd) 543.117 (obsd). Anal. Calcd for $C_{30}H_{25}BN_2S_3$: C, 69.22; H, 4.84; N, 5.38. Found: C, 69.92; H, 4.79; N, 5.19.

Synthesis of ***2b*** *[3,4,4-Tri(5-R-(2-thienyl))-8-(2,4,6-R′-phenyl)-4-bora-3a,4a-diaza-s-indacene (R = R′ = Me)].* The synthesis of compound **2b** was similar to that for compound **2a**. First, 2-methylthienyllithium was prepared separately. 2-Methylthiophene (0.63 mL, 6.4 mmol) was dissolved in anhydrous THF (10 mL) before being allowed to undergo reaction with *n*-BuLi (2.6 mL, 2.5 M in THF) at −78 °C for 10 min. The reaction mixture was then allowed to warm to ambient temperature.[38] After this procedure, this THF solution was transferred into a solution of compound **2** (0.50 g, 1.6 mmol in 20 mL THF). After the workup process, compound **2b** was isolated via recrystallization out of methanol (0.65 g, 70%). ^{1}H NMR spectral signals ($CDCl_3$: δ 7.24, 400 MHz): δ 7.61 (t, $^3J_{H-H}$ = 1.5 Hz, $1H_h$), 7.02 (s, $2H_b$), 6.92 (d, $^3J_{H-H}$ = 3.2 Hz, $2H_l$), 6.90 (d, $^3J_{H-H}$ = 3.8 Hz, $1H_i$), 6.79 (d, $^3J_{H-H}$ = 4.5 Hz, $1H_e$), 6.75 (d, $^3J_{H-H}$ = 4.5 Hz, $1H_d$), 6.65 (dd, $^3J_{H-H}$ = 3.2 Hz, $^4J_{H-H}$ = 1.0 Hz, $2H_m$), 6.56 (dd, $^3J_{H-H}$ = 4.2 Hz, $^4J_{H-H}$ = 1.2 Hz, $1H_f$), 6.49 (dd, $^3J_{H-H}$ = 3.8 Hz, $^4J_{H-H}$ = 1.0 Hz, $1H_j$), 6.36 (dd, $^3J_{H-H}$ = 4.1 Hz, $^3J_{H-H}$ = 1.8 Hz, $1H_g$), 2.48 (d, $^4J_{H-H}$ = 0.5 Hz, $6H_{n'}$), 2.42 (s, $3H_{c'}$), 2.40 (s, $3H_{k'}$), 2.20 (d, $^4J_{H-H}$ = 4.6 Hz, $6H_{a'}$). ^{13}C NMR spectral signals ($CDCl_3$: δ 53.8, 100 MHz): δ 152.1 (td, $^1J_{C-H}$ = 8.8 Hz, $^2J_{C-H}$ = 2.5 Hz, $1C_5$), 150.5 (br, $1C_7$), 143.5 (dt, $^1J_{C-H}$ = 183.1 Hz, $^2J_{C-H}$ = 8.8 Hz, $1C_h$), 143.5 (m, $1C_6$), 140.7 (m, $2C_n$), 138.2 (m [*looks like: q,* $^2J_{C-H}$ *5.9 Hz*], $1C_c$), 136.9 (m, $1C_3$), 136.7 (m, [*looks like: q,* $^2J_{C-H}$ *= 5.7 Hz*] $2C_a$), 132.8 (dd, $^1J_{C-H}$ = 169.1 Hz, $^2J_{C-H}$ = 6.0 Hz, $1C_i$), 132.7 (m, [*looks like: q,* $^2J_{C-H}$ *= 8.6 Hz*] $1C_4$), 132.04 (m, $1C_k$), 131.1 (br, $1C_1$), 130.1 (dd, $^1J_{C-H}$ = 161.1 Hz, $^2J_{C-H}$ = 6.0 Hz, $2C_l$), 128.9 (dd, $^1J_{C-H}$ = 174.1 Hz, $^2J_{C-H}$ = 3.5 Hz, $1C_e$), 128.1 (dm, $^1J_{C-H}$ = 146.2 Hz, $2C_b$), 126.4 (dm, $^1J_{C-H}$ = 165.0 Hz, $1C_j$), 125.6 (dm, $^1J_{C-H}$ = 169.8 Hz, $3C_{m,f}$), 121.6 (dd, $^1J_{C-H}$ = 173.1, $^2J_{C-H}$ = 3.6 Hz, $1C_d$), 117.7 (dd, $^1J_{C-H}$ = 173.5 Hz, $^2J_{C-H}$ = 8.8 Hz, $^2J_{C-H}$ = 3.0 Hz, $1C_g$), 21.2 (dd [*looks like: q*], $^1J_{C-H}$ = 125.4 Hz, $^3J_{C-H}$ = 4.4 Hz, 1C), 20.0 (q, $^3J_{C\_-H}$ = 5.0 Hz, $1C_{a'}$), 15.4 (qd, $^1J_{C-H}$ = 127.2 Hz, $^3J_{C-H}$ = 2.4 Hz, $2C_{n'}$, $1C_{k'}$). ^{11}B NMR spectral signals ($CDCl_3$, $BF_3 \cdot OEt_2$: δ 0.00, 128 MHz): δ −3.01 (s). MALDI-TOF *m/z* (M^+): 562.17 (calcd), 561.65 (obsd). HRMS *m/z* ($(M + Na)^+$): 585.164 (calcd), 585.164 (obsd).

Synthesis of ***3a*** *[3,4,4-Tri(2-thienyl))-8-phenyl-4-bora-**3a**,**4a**-diaza-s-indacene].* All processes undertaken to obtain compound **3a** were analogous to those for the synthesis of **1a**,[18] except for the use of compound **3** (0.4 g, 1.5 mmol) in place of compound **1**. A portion of 2-thienyllithium (6.0 mL, 1.0 M in THF) was added. Finally, compound **3a** was isolated via recrystallization out of methanol (0.1 g, 14%). ^{1}H NMR spectral signals (CD_3COCD_3: δ 2.05, 400 MHz) are as follows: δ 7.69 (m, $2H_a$), 7.66 (m, $2H_b$), 7.62 (m, $^3J_{H-H}$ = 1.43 Hz, $1H_c$), 7.60 (m, $^3J_{H-H}$ = 1.6 Hz, $1H_h$), 7.40 (dd, $^3J_{H-H}$ = 5.1, $^4J_{H-H}$ = 1.1 Hz, $1H_i$), 7.32 (dd, $^3J_{H-H}$ = 4.8, $^4J_{H-H}$ = 1.0 Hz, $2H_n$), 7.14 (d, $^3J_{H-H}$ = 4.4 Hz, $1H_d$), 7.04 (dd, $^3J_{H-H}$ = 3.4 Hz, $^4J_{H-H}$ = 1.0 Hz, $2H_l$), 6.93 (dd, $^3J_{H-H}$ = 3.4 Hz, $^4J_{H-H}$ = 1.5 Hz, $2H_m$), 6.92 (m, $1H_e$), 6.90 (dd, $^3J_{H-H}$ = 3.7 Hz, $^4J_{H-H}$ = 1.1 Hz, $1H_k$), 6.86 (dd, $^3J_{H\_H}$ = 4.3 Hz, $^4J_{H-H}$ = 1.2 Hz, $1H_f$), 6.75 (dd, $^3J_{H-H}$ = 5.1 Hz, $^3J_{H-H}$ = 3.8 Hz, $1H_j$), 6.50 (dd, $^3J_{H-H}$ = 4.3 Hz, $^3J_{H-H}$ = 1.9 Hz, $1H_g$). ^{13}C NMR spectral signals (CD_3COCD_3: δ 30.0, 100 MHz): δ 152.9 (m, $1C_5$), 145.7 (s, $1C_2$), 145.3 (dt, $^1J_{C-H}$ = 183.6, $^2J_{C-H}$ = 8.9 Hz, $1C_h$), 137.5 (m, [*looks like: t,* $^2J_{C-H}$ *= 8.8 Hz*] $1C_3$), 135.3 (m, $1C_1$), 134.9 (m, $1C_6$), 133.7 (m, [*looks like: q,* $^2J_{C-H}$ *= 8.7 Hz*] $1C_4$), 132.5 (dm, $^1J_{C-H}$ = 169.5 Hz, $1C_k$), 131.5 (dm, $^1J_{C-H}$ = 178.6 Hz, $1C_d$), 131.3 (dm, $^1J_{C-H}$ = 170.2 Hz, $2C_l$), 131.2 (dm, $^1J_{C-H}$ = 172.3 Hz, $2C_b$), 131.1 (dm, $^1J_{C-H}$ = 180.9 Hz, $2C_a$), 129.8 (dm, $^1J_{C-H}$ = 186.1 Hz, $1C_i$), 129.3 (dm, $^1J_{C-H}$ = 200.4 Hz, $1C_c$), 128.8 (dm, $^1J_{C-H}$ = 173.7 Hz, $1C_f$), 128.0 (dm, $^1J_{C-H}$ = 168 Hz, $1C_j$), 127.9 (dm, $^1J_{C-H}$ = 170.7 Hz, $2C_m$), 127.4 (dm, $^1J_{C-H}$ = 164.9 Hz, $2C_n$), 122.7 (dd, $^1J_{C-H}$ = 172.0 Hz, $^2J_{C-H}$ = 5.4 Hz, $1C_e$), 119.1 (ddd, $^1J_{C-H}$ = 174.0 Hz, $^2J_{C-H}$ = 8.7 Hz, $^2J_{C-H}$ = 3.8 Hz, $1C_g$). ^{11}B NMR spectral signals (CD_3COCD_3, BF_3OEt_2: δ 0.00, 128 MHz): δ −1.99 (s). HRMS *m/z* ($(M + Na)^+$): 501.070 (calcd), 501.067 (obsd). Anal. Calcd for $C_{27}H_{19}BN_2S_3$: C, 67.78; H, 4.00; N, 5.85. Found: C, 66.63; H, 4.13; N, 5.64.

X-ray Structure Determinations. High-quality crystals of compounds **2a**, **2b**, and **3a** were grown from methanol. Single crystals of appropriate sizes were selected and mounted on a goniometer by standard methods at room temperature. Data were collected on a Bruker P4 diffractometer equipped with a SMART CCD detector. Crystal data, data collection, and refinement parameters are provided in the Supporting Information. The molecular structures were elucidated using direct methods and standard difference map techniques to "solve" the structure; full-matrix least-squares refinement procedures were performed on F^2 values with the SHELXTL program (version 5.10).[39] Some of the thienyl moieties were found to be crystallographically disordered as evidenced by distortions in the atomic thermal parameters upon preliminary least-squares refinement of the full initial solution. Two ring conformations clearly exist and are related by a rotation of ca. 180° about their respective $C_{dipyrrin}-C_{thienyl}$ or $B-C_{thienyl}$ vectors. Such disorder was previously encountered in related dipyrromethane and BF_2-dipyrrin derivatives.[18,35] This disorder was modeled here, as before, by creating atomic coordinates for a second thienyl group; both "parts" were satisfactorily least-squares refined. The hydrogens on the solvent carbon atoms were not added. The *.cif files of crystallographic determinations have been deposited with the Cambridge Crystallographic Data center (CCDC 788639 (**3a**) and 788640 (**2a**)). These data are available at www.ccdc.cam.ac.uk/conts/retrieving.html or from the CCDC, 12 Union Road, Cambridge CB2 IEZ, United Kingdom; fax +441223-336033; e-mail: deposit@ccdc.cam.ac.kr. The X-ray structure of **2b** was determined tentatively as well, but this data is not included here.

Computational Details. The Gaussian 03 program[40] was used for all calculational work provided in the Supporting Information. All geometries were processed in silico in the gas phase at 0 K. Hardware used involved an in-house Intel Pentium IV 3.0 system. Molecular orbital images were obtained through the use of Gauss View 3.0. This following protocol was used for all calculations: (i) input geometries were prepared from the crystallographic atomic coordinates where possible or by careful modification of closely related geometries by scientific graphics software and invoking chemical intuition. (ii) Density functional theory (DFT) geometry optimizations were performed at the B3LYP level[41,42] with a combination of basis sets: Lanl2DZ[43] for Cu; 6-31G(d)[44] for N and S; 3-21G[45] for C, H, B, and F. (iii) Vibrational frequencies were determined for all geometries, and negative ones were found to be absent signifying that a true minimum was found.

Isothermal Titration Calorimetry (ITC) Binding Studies. A VP-ITC instrument manufactured by MicroCal, Inc. was used to determine the molar enthalpy (Δ*H*) of complexation. Titrations were performed at 25 ± 0.01 °C. Blank titration samples were also measured in plain solvent, and this data was subtracted from the corresponding titration so as to remove from consideration any effect associated with heats of dilution involving the titrant. The actual experiment consisted of filling the sample cell with a host solution, filling the syringe with a solution of $HgClO_4$, and titrating via a computer-automated injector. Subsequent fitting of the data to a 1:1 binding profile using the included Origin software package provided access to the association constant K_a and differences in entropy Δ*S*, enthalpy Δ*H*, and thus Gibbs free energy (Δ*G*).

RESULTS AND DISCUSSION

Three new BODIPY "scorpionate"-like species **2a**, **2b**, and **3a** were synthesized in accordance with previous synthetic protocols (Scheme 1)[18] and fully characterized by various methods

dx.doi.org/10.1021/ic101681h |*Inorg. Chem.* 2011, 50, 5351–5360

Scheme 1. (Top) Structures of Related Compounds That Have Been Previously Reported.[18,35] (Bottom) Preparation of "Scorpionate-Like" BODIPY Derivatives and the Positions of Methylation[a]

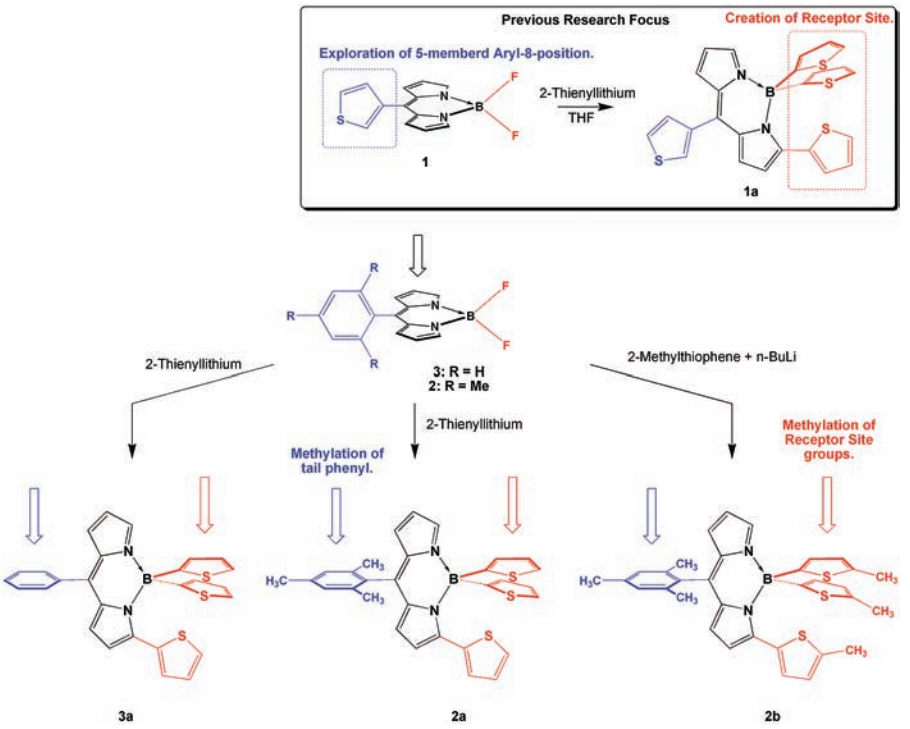

[a] THF was used as a solvent at -78 °C for the salt metathetic reaction that forms compounds **2a**−**3a**.

(vide infra). While they can be commonly referred to as dipyrrin species, rigorous boradiazaindacene complex naming is also customary and preferred by some practioners: 3,4,4-tris(5-R-(2-thienyl))-8-(2,4,6-R′-phenyl)-4-bora-3a,4a-diaza-*s*-indacene (R, R′ = H, **3a**; R = H, *R*′ = Me, **2a**; R = Me, R′ = Me, **2b**). These three compounds are the first 8-phenylscorpionate-type derivatives to be synthesized.[18] The synthesis of the BF_2 derivatives **3** and **2** was performed as previously reported[46] and was analogous to that for **1**. Chromatography was used extensively for purification purposes again, analogous to what was described before for related species. The pure products are easily characterized by their bright red appearance, fluorescence (TLC assays), and respective mass spectrometric (*m*/*z*) values of 520.64, 561.65, and 478.32 that correlate well with the respective calculated values. With various 1-D and 2-D NMR spectroscopic techniques, the purity of **2a**, **2b**, and **3a** can be determined. While the methyl groups for **2a** and **2b** are easily assigned, conformation and assignment of the sp^2-hybridized carbon resonances were also possible. While some ^{1}H assignments were made conveniently by analogy to those reported previously in closely related sytems,[22] some differences exist here. First, we simply demonstrated that boron was present; support in solution for boron in **2a**, **2b**, and **3a** comes from the clear assignable singlets in the ^{11}B NMR spectra, respectively, at δ −2.00, −3.01, and −1.99 ppm (see the Supporting Information for reproductions of these and all other spectra). Next, in ^{1}H and ^{13}C NMR spectra, the overall correct number of peaks is present, according to the structures provided in Scheme 1. Further, the requisite number of cross-peaks in the 2-D ^{1}H−^{1}H COSY spectra exists, as well (Supporting Information). Also, the ^{1}H−^{13}C HMQC spectra conveniently show cross peaks for the correct number of anticipated protons. Lastly, the quaternary carbons were further scrutinized with the help of ^{1}H−^{13}C HMBC NMR spectra (see the Supporting Information).

Optical Properties. Compounds **2a**−**3a** are red green (dichroic) crystalline solids stable on the bench-top as powders in (moist) air for more than one year. Dissolution of these complexes into various solvents gives rise to green fluorescent red solutions, characteristic for BODIPY systems. The principal optical features are revealed in Figure 2 (properties are tabulated in the Supporting Information). Briefly, the original brilliant fluorescence intensity for **2** (Φ_F = 0.93, toluene)[32] carries over partly to **2a** (Φ_F = 0.27 ± 0.013, acetonitrile). Compound **2a**, which is by far the most fluorescent of the three, is shown in solution (photographs, Figure 2); it is promising in that closely related systems were soluble in 50% water (MeCN/H_2O, 50:50 by vol.).[35] Formal incorporation, or removal, of methyl groups gives **2b** (Φ_F = 0.024 ± 0.0016) and **3a** (Φ_F = 0.0034 ± 0.00047). The Ph/mesityl 8-substitution difference in these "scorpionate-like" units is parallel to that difference between the parent difluoroboryl species: Φ_F = 0.053-0.062 vs 0.93 (toluene).[32] Interestingly, **2b** is weakly fluorescent. Why methylation at the "head" thienyl groups for **2b** gives a formal decrease in Φ_F value might be rationalized by the fact that the methyl groups enhance non-radiative pathways directly or may constrain highly emissive conformations. In any event, the fluorescence lost by such formal thienyl substitution can be retrieved upon selective heavy atom binding (chelation-enhanced fluorescence), as observed in the **1a**·Cu^{2+} case in which the Φ_F value of the fluorophore complex increased dramatically from 0.012 to 0.194.[18]

Optical Changes upon M^{n+} titration. A range of metal ions was used for **2a**−**3a** in screening for M^{n+} recognition as performed

dx.doi.org/10.1021/ic101681h |*Inorg. Chem.* 2011, 50, 5351–5360

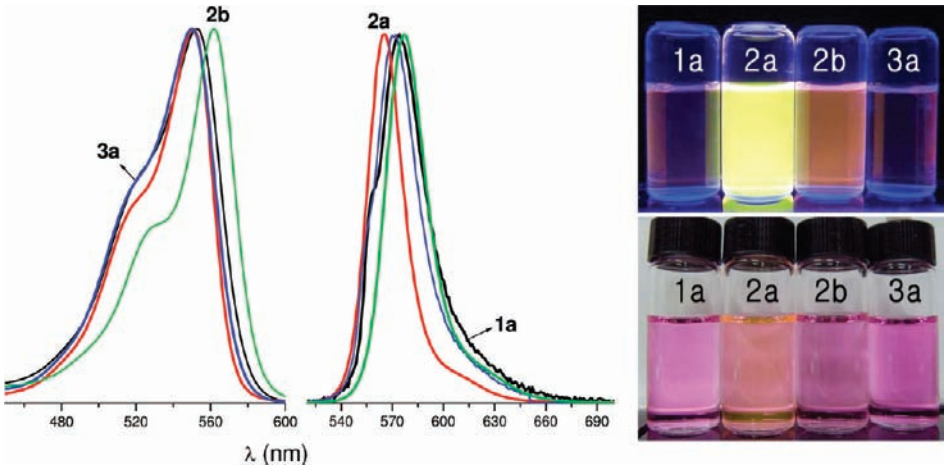

Figure 2. (Left) Normalized UV-vis absorption and emission spectra and (upper right) photos of four species (**1a**, **2a**, **2b**, and **3a**) under UV irradiation (365 nm) in acetonitrile. (Lower right) The same vials and samples shown under white light: 10 μM. The tetrathienyl-containing species **1a** is used as a reference.[18]

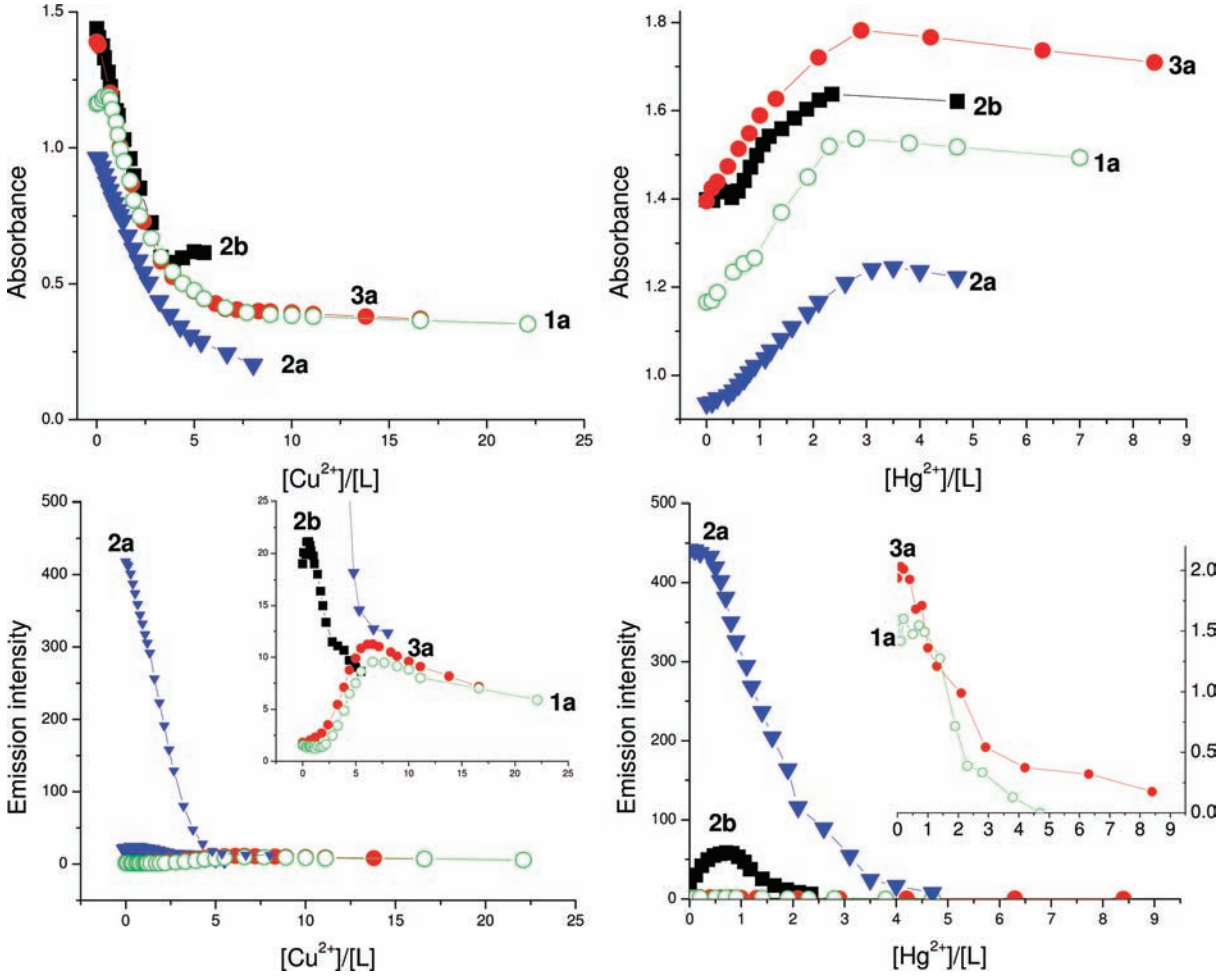

Figure 3. Full plots of $\lambda_{abs,max}$ and $\lambda_{em,max}$ values as a function of equivalents of analyte. Changes of the absorbance and emission intensity are shown upon Cu^{2+} and Hg^{2+} titration with compounds **1a**−**3a**. **1a**−**3a** = 2.68×10^{-5} M; Cu^{2+} = 4.45×10^{-3} M; Hg^{2+} = 3.78×10^{-3} M, acetonitrile solvent. UV−vis and emission spectra were acquired immediately after sample preparation.

previously for similar BODIPY species.[47] The perchlorates of Cu^{2+} and Hg^{2+} were used and led to UV−vis and emission spectral changes shown in Figure 3; photos of the vials are shown in Figure 4. The emission spectral changes upon addition of titrants are as follows: **2a**, which is greatly fluorescent, loses its fluorescence evenly and significantly between 0 and 3 equiv of

dx.doi.org/10.1021/ic101681h |*Inorg. Chem.* 2011, 50, 5351–5360

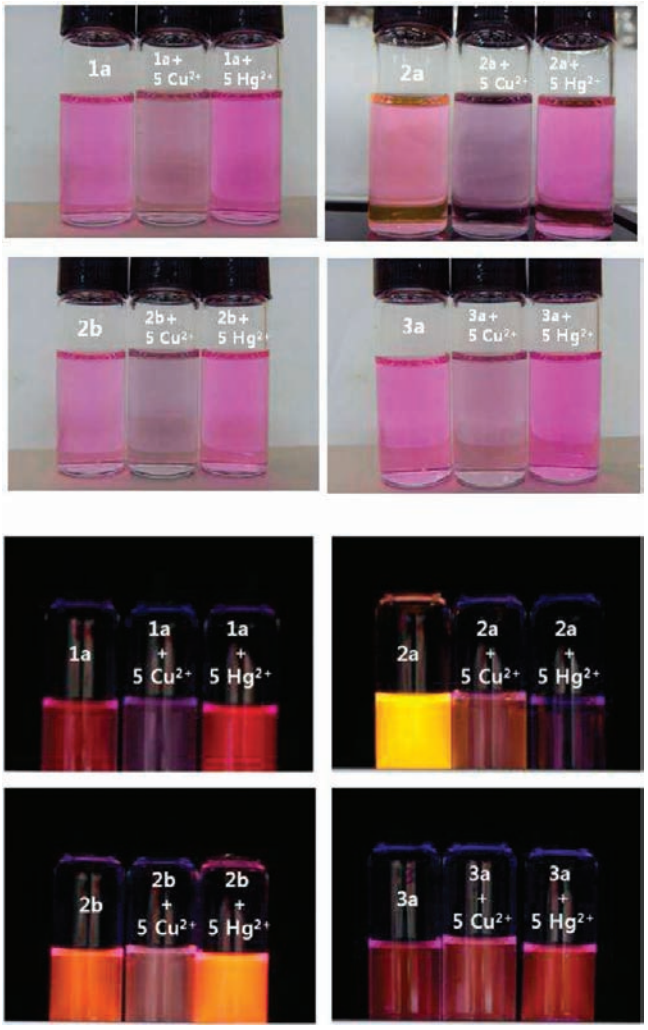

Figure 4. Digital photos of **1a**−**3a** in acetonitrile solution after addition of 5 equiv of metal ion: (top) naked eye detection; (bottom) use of fluorescence (lamp with bulb giving emission at 365 nm). Concentrations of ligand (10 μM), Cu^{2+} (50 μM), and Hg^{2+} (50 μM).

titrant. This tailing off of fluorescence intensity after 3 equiv leads to very little remaining fluorescence at 5 equiv. This trait is found for both ions Cu^{2+} and Hg^{2+}. The behavior of **2b** starts with a very small increase between 0 and 1 equiv of Cu^{2+} titrant, followed by a general turn-off behavior until equiv ~5 (where the measurement stopped). This same species responds in a "turn-on" fashion when in the presence of Hg^{2+}, giving the essential opposite effects, differences that signify the essence of this study. Further, compound **3a** gives a "turn-on" response from 0 to 5.5 equiv of Cu^{2+} titrant and allows for a 6.3-fold increase, reaching saturation at ~5.5 equiv of Cu^{2+}; a "turn-off" response is then seen from 5.5 to 16 equiv of Cu^{2+}. For **3a** with Hg^{2+}, however, there is a direct "turn-off" response starting from 0 to 3 equiv. This fluorescence increase found here for Hg^{2+} through methyl substitution is significant, considering the various photophysical quenching mechanisms possible for this ion when in contact with fluorogenic groups.[11] Even at higher equivalency, the onset of potential *collisional* quenching due to the increase in the concentration of Hg^{2+} is very gradual. For example, in the mixture of **3a** + Hg^{2+}, the reliability in the fluorescence detection signal appears to exist over the course of hours and days in this assay.

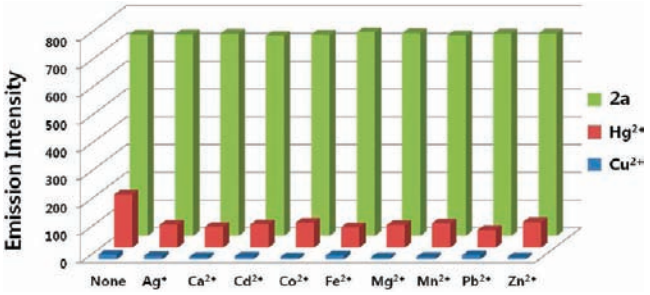

Figure 5. Emission intensity of **2a** (5.0×10^{-6} M, green bars) with 5 equiv of Cu^{2+} (blue bars) or Hg^{2+} (red bars) with various metal ions (10 equiv) in acetonitrile.

Colorimetrically, in the UV−vis spectra (Figure 3, top) there is "turn-off" optical behavior for all species (**2a**, **2b**, and **3a**) with Cu^{2+}. Saturation occurs generally in the range of 5−7 equiv of Cu^{2+}. For Hg^{2+}, there is a "turn-on" response for all species (**1a**−**3a**) to about 2−3 equiv. Compounds **2a** and **3a**, along with the previously measured **1a**, have larger λ_{max} absorbance increases, whereas **2b** gives a more modest increase. Due to the natural brightness of color, we examined the colorimetric capabilities at *low* concentration, stepping down by factors of 10 in concentration from what were described above (Figure 3). The limits of detection in compounds **2a**−**3a** for Cu^{2+} and Hg^{2+} were calculated. For Cu^{2+}, compounds **2a**, **2b**, and **3a** have the values of 1.2, 0.71, and 1.6 μM, respectively. For Hg^{2+}, the values are 1.6, 1.6, and 2.2 μM, respectively. Binding constants were also obtained from these spectrometric titration results. The values obtained are as follows: $1.10 \times 10^4 \pm 1170$ M^{-1} for **2a**···Cu^{2+}, $4.18 \times 10^3 \pm 1080$ M^{-1} for **2b**···Cu^{2+}, and $2.92 \times 10^4 \pm 4050$ M^{-1} for **3a**···Cu^{2+}.

Next, we determined the selectivity of metal ions for receptor **2a**. Compound **2a** can be considered as a formal intermediate when considering its degree of methyl substitution compared to that for derivatives **2b** and **3a**. Specifically, solution metal ion sensing competition studies were performed with Cu^{2+} and Hg^{2+} versus other available various metal cations (Ag^+, Ca^{2+}, Cd^{2+}, Co^{2+}, Fe^{2+}, Mg^{2+}, Mn^{2+}, Pb^{2+}, and Zn^{2+}) (Figure 5). After the addition of 5 equiv of Cu^{2+} to compound **2a**, the fluorescence was quenched. In the presence of 10 equiv of other metal ions, the solutions of **2a** still gave high fluorescence. However, after the addition of 5 equiv of Cu^{2+} to **2a**−metal ion mixture, the fluorescence was again quenched. These results mean that Cu^{2+} ion binding to **2a** is predominant over the other metal ions (blue bars). This phenomenon also occurs for the Hg^{2+} ion case in which fluorescence quenching occurs in the presence of other metal ions (red bars) but to a lesser extent than for Cu^{2+}.

In the presence of *both* Cu^{2+} and Hg^{2+}, the **2a** compound solution (acetonitrile) absorption spectrum shows a predictable $\lambda_{abs,max}$ decrease at 551 nm (see the Supporting Information). This observation is the same as the consequence of **2a**···Cu^{2+} binding; **2a**···Hg^{2+} binding is typically evidenced by a new absorbance $\lambda_{abs,max}$ peak at 543 nm, but there was no appearance of this peak. Therefore, Cu^{2+} binding with compound **2a** is more dominant than that for Hg^{2+}, even though a higher Hg^{2+} concentration is present.

Job Plots, DFT Geometry Optimization Calculations, Binding Thermodynamics, and ^{1}H NMR Spectroscopic Studies. The optical changes presented and discussed so far allow for

dx.doi.org/10.1021/ic101681h |*Inorg. Chem.* 2011, 50, 5351–5360

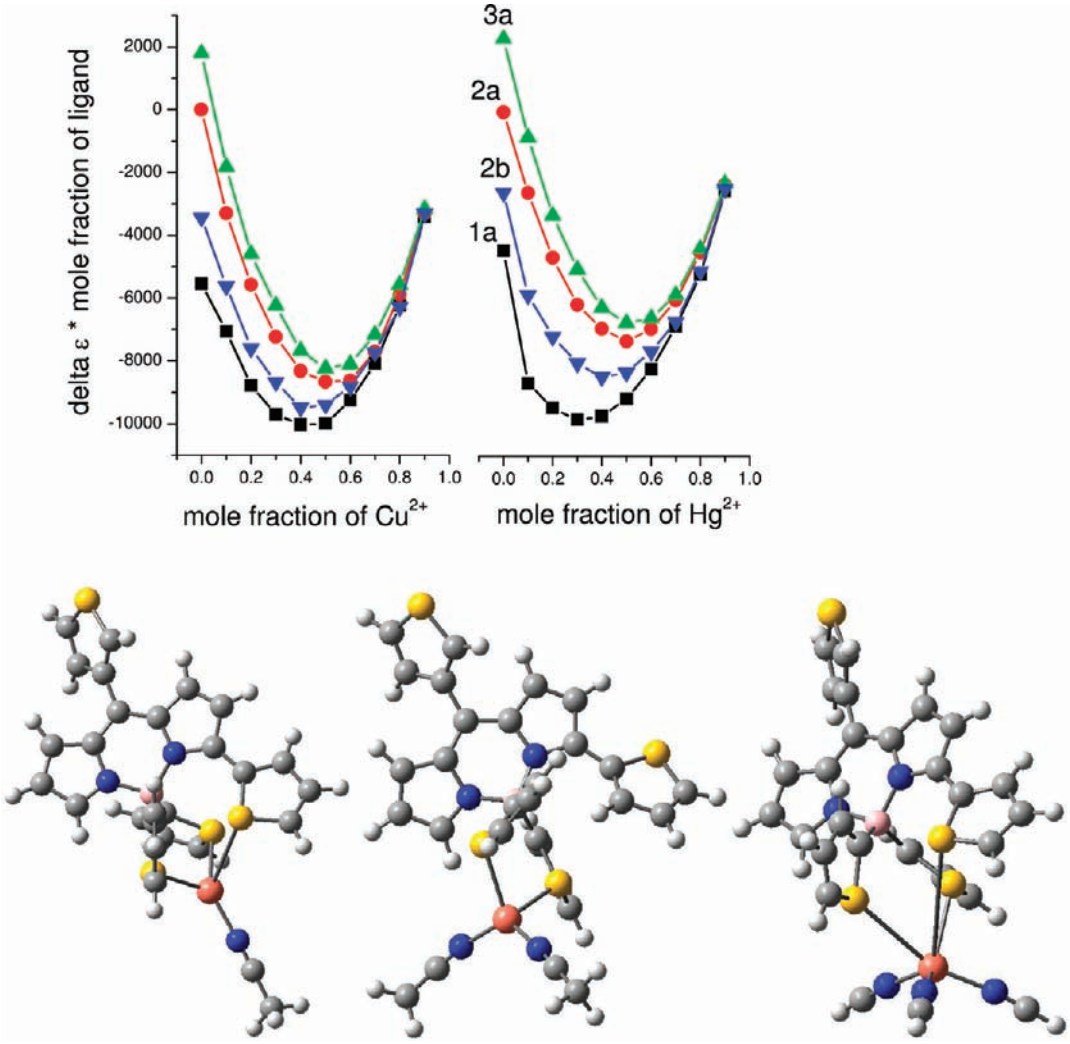

Figure 6. (Top) Job plot analysis for ligands **1a**, **2a**, **2b**, and **3a** with Cu^{2+} (top left) and Hg^{2+} (top right). *Y*-axis of graph = $\Delta(\varepsilon - \varepsilon_0) \times$ mole fraction of receptor (**1a**−**3a**) (ε: absorption coefficient of ligand with target ions, ε_0: absorption coefficient of ligand without target ions). (Bottom) Geometric structures from high-level DFT geometry optimization calculations of compound **1a** showing variations of Cu^{2+} binding into the [*SSS*] core with 1, 2, or 3 corresponding coordinated MeCN solvent molecules (gray = carbon, yellow = sulfur, blue = nitrogen, red-orange = copper).

various further analysis through the use of other techniques. Namely, (i) Job plots for **1a** and **2a**−**3a**, (ii) DFT geometry optimization calculations of **1a**-Cu^{2+}, (iii) binding thermodynamics for **2a** using ITC measurements, and (iv) ^{1}H NMR spectroscopic evidence of complex formation with **2b** were obtained. An analysis of metal ion binding by Job's method appears in Figure 6 (top). For the three complexes, the various stoichiometries were determined: **1a**:Cu^{2+} = 3:2 or 1:1, **2a**:Cu^{2+} = 1:1, **2b**:Cu^{2+} = 1:1 or 3:2, **3a**:Cu^{2+} = 1:1, **1a**:Hg^{2+} = 2:1, **2a**:Hg^{2+} = 1:1, **2b**:Hg^{2+} = 3:2 or 1:1, **3a**:Hg^{2+} = 1:1. The occasional discrepancy from 1:1 suggests that the ligand might occasionally form a sandwich compound (L···M^{2+}···L) or some different unanticipated chelation forms in solution.

Interestingly, these molecules have recognition for Cu^{2+} and Hg^{2+} in acetonitrile through the use of the 2-thienyl pocket which accommodates a simple metal ion in both cases of Cu^{2+} and Hg^{2+}. However, the thienyl group at the 8-position might also interact with guest cations, as reflected by compound **1a** having a hypothetical binding stoichiometry of ~3:2 for Cu^{2+} or even a value of 2:1 for Hg^{2+}. We also considered the methyl effect in the [SSS] pocket toward metal ion sensing. Through Job's plot analysis, compound **2b** showed a ~1:1 (or perhaps a ~3:2) binding stoichiometry which accounted for the fluorescence emission saturation patterns observed spectrally for **2b** with both metal ions (Cu^{2+} and Hg^{2+}) (Figure 3). Compound **2b** shows fluorescence emission saturation for both Cu^{2+} and Hg^{2+} distinctively different from what we would predict from the straightforward [SSS] pocket binding structure of **2a** as shown for Cu^{2+}···**1a** (Figure 6). It is likely that the methyl-substituted [SSS] pocket provides a more sterically hindered site for certain metal ions; the mesityl group at the 8-position might also place further sterical obligations on the conformations necessary for chelation in the "head" area. Because of these geometrical properties, enhanced emission could arise from a process whereby the methyl groups attached to the thienyl rings are locked out of certain conformations until metal chelation is effected, which then gives chelation enhanced fluorescence (CHEF) as observed in the "turn-on" responses found for Hg^{2+} with **2b**.

Separately, DFT calculations were undertaken to try to analyze the proposed binding site at the atomic level when engaged in

dx.doi.org/10.1021/ic101681h |*Inorg. Chem.* 2011, 50, 5351–5360

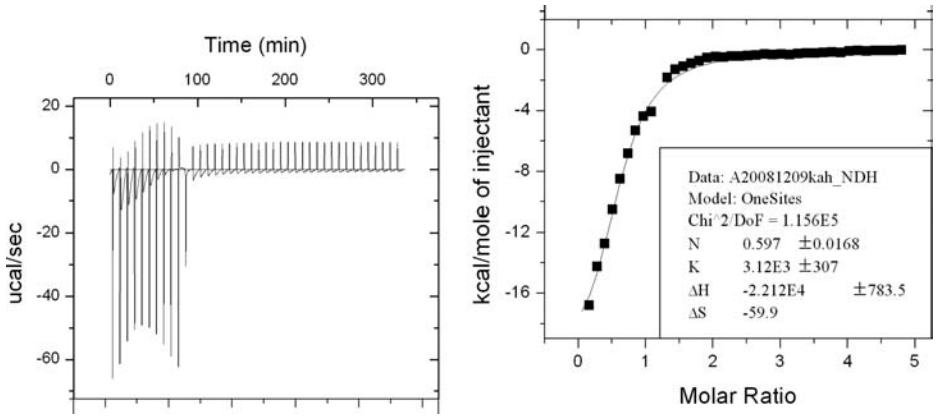

Figure 7. (Left) ITC measurements of **2a** (3.85 mM) with $Hg(ClO_4)_2$ in acetonitrile at 25 °C. Plot of μcal/s values obtained for times 0−330 min. (Right) Plot of changes in kcal mol^{-1} as a function of injectant in which K_a was determined as 3120 ± 307 M^{-1}.

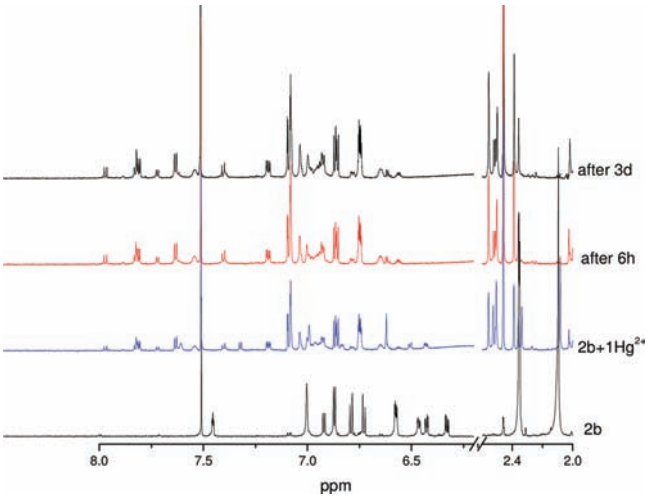

Figure 8. Stack-plot of ^{1}H NMR spectra for the treatment of **2b** with Hg^{2+} at 5.2 × 10^{-3} M concentration. See the Supporting Information for more data.

metal binding. The input **1a** structures of complexes [[S,S,S]·Cu^{2+}·MeCN] [[S,S]·Cu^{2+}·2MeCN] and [[S,S,S]·Cu^{2+}·3 MeCN] were prepared in silico from structural coordinates of the ligand and were subjected to theoretical geometry optimization. Their fully optimized molecular structures appear in Figure 6 (bottom). A preliminary molecular orbital analysis was also performed and is included in the Supporting Information. These complexes show that the metal ion sits quite stable in the [SSS] pocket along with a certain designated number of manually oriented η-1-bound MeCN solvent molecules. The computational stability of these fragments further supports the existence of a believably versatile coordination pocket. Interestingly, the tridentate chelation leads to a "chiral propeller"-type arrangement of the thienyl substituents.

In further considering the [*SSS*] binding site for these compounds, ITC methods were explored for the association of **2a** with Hg^{2+} in solution at mM concentration (Figure 7). An equilibrium value (K_a) for the association was determined to be 3120 ± 307 M^{-1}. The values for ΔH (−2.212 × 10^4 ± 783.5 kcal mol^{-1}) and ΔS (−60 eu) were also obtained directly.

Changes are seen to arise from a related set of ^{1}H NMR spectrosopic studies involving **2a**−**3a** in M^{2+} titrations. In a sealed J. Young tube for NMR spectroscopy (constant solution volume) [CD_3CN:$CDCl_3$ = 2:1 by volume] with 0.0052 M concentration of Cu^{2+} and Hg^{2+} and a 0.0052 M concentration of **2b**, new peaks appear in the Hg^{2+} sample, tentatively assigned to Hg^{2+}·**2b**. For Hg^{2+}, there are instant dramatic changes in which, e.g., ligand peaks at δ 6.5−7.5 are completely consumed upon addition of Hg^{2+} (Figure 8); new peaks in the range of 6.3−8.0 appear in line with discrete pyrrolyl and thienyl peaks arising from particular interactions with the metal ion. The loss in concentration of **2b** is not concomitant with the growth of new signals in the ^{1}H NMR spectrum. Overall, a loss of detectable species is apparent (increased relative noise). Some new clear peaks exist for the Cu^{2+} sample; there appear to be some paramagnetic species forming as well. Unfortunately, at longer times, there is some evidence of peaks assigned to free thiophene. Thus, while there may be (in)stability issues at higher concentration, when considering Cu^{2+}, there is sufficiently clear information early in the titration when considering the Job plots and the ITC measurement data that point to complex stability at shorter times.

Structural Data of 2a and 3a. Crystals of **2a** and **3a** were obtained for X-ray diffraction through their growth and precipitation out of methanol solution. The molecular structures of **2a** and **3a** were obtained via single-crystal X-ray diffraction in space groups *C*2/*c* and $P2_1/n$, respectively (Figure 9, top and middle). All bond distances and angles are provided in the Supporting Information. A tentative crystal solution of **2b** was also obtained but is not included herein. The molecular structures for **2a** and **3a** confirm the proposed structures strongly supported by various types of solution NMR spectroscopy (vide supra). Namely, the presence of three, and not four, thienyl groups at the "head" position was confirmed. The isolation of an impurity product bearing four thienyl groups (3,4,4,5-tetrathienyl) is possible; careful separation via PTLC is thus required. In **2a** and **3a**, the many aryl groups allow for a consideration of angles between the calculated mean planes (Figure 9, bottom). Most such dihedral angles are not discussed here in deference to limiting the Discussion to the most important aspects. Importantly, the most telling interplanar angle is that for the 8-position angle: the dihedral angle between the BODIPY main framework (N1, N2, C1−C9) and the aryl ring (non-H) atoms is 75.4° for **2a**, 80.8° for **2b**, and 60.7° for **3a**. Another issue related to metal binding is whether the "head" thienyls are either *preorganized* or *predisposed* toward metal chelation. It is sterically reasonable, however, to have the sulfurs pointing toward each other, so as to minimize thienyl methine group congestion and collisions. However, solid-state

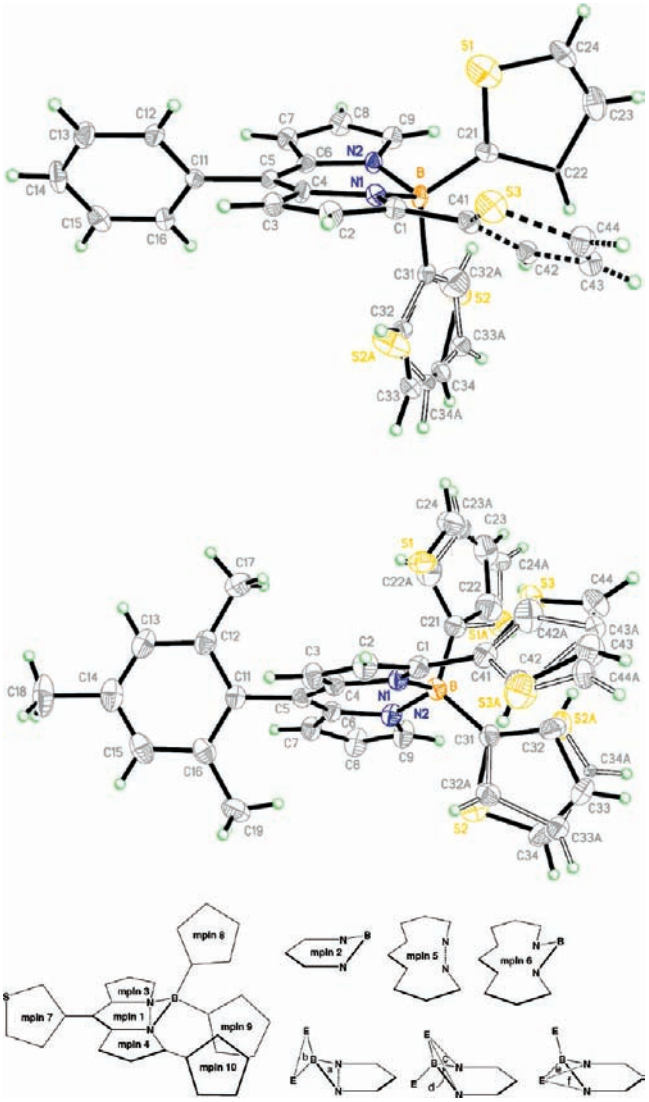

Figure 9. Molecular structures of compounds **3a** (top) and **2a** (middle). Ellipsoids are drawn at 20% probability. (Bottom) The various mean planes (mplns) for the dipyrrin species discussed herein. **3a**: CCDC 788639; $P2_1/n$, unit cell parameters: a = 8.5287(6) Å, b = 9.1106(7) Å, c = 30.020(2) Å, β = 95.135(5)°. **2a**: CCDC 788640; $C2/c$, unit cell parameters: a = 17.2235(18) Å, b = 21.909(2) Å, c = 16.217(3) Å, β = 115.963(3)°.

analysis reveals no particular conformer arrangement when considering one BODIPY molecule at a time (not a packing scheme); in fact, the observed conformations might arise from simple crystal packing requirements with neighboring molecules. Separately, the obliqueness of mean plane 10, relative to mean plane 4 (or mean planes 5 and 6) might influence electronic delocalization. If mean planes 10 and 4 remain coplanar, which could occur upon metal ion binding, such resulting electron delocalization may thus create different electronic and thus could be related to the observed fluorescence properties and fluorescence switching patterns.

CONCLUSION

Herein, we report the synthesis, multinuclear NMR spectroscopic characterization, crystallographic structural characterization, high-resolution mass spectrometry, and theoretical calculations of three new closely-related thienyl-derivatized scorpionate BODIPY-type species [3,4,4-tris(5-R-(2-thienyl))-8-(2,4,6-R′-phenyl)-4-bora-3a,4a-diaza-*s*-indacene (R, R′ = H, **3a**; R = H, R′ = Me, **2a**; R = Me, R′ =Me, **2b**)]. We have discovered that, to the best of our knowledge for the first time in fluorophore chemistry, very minor substituent (i.e., Me → H; H → Me) directing "turn-on" or "turn-off" fluorescence intensity behavior at low concentration with metal ions. This characterization and analysis was done in the context of Cu^{2+} and Hg^{2+} solution detection. The limits of detection were calculated to be in the range of 0.7−1.6 μM for Cu^{2+} and 1.6-2.2 μM for Hg^{2+}. An understanding of receptor binding has been characterized by Job plot analysis, ITC (isothermal titration calorimetry) measurements, DFT calculations, and ^{1}H NMR spectrotitrimetric analysis. Through our study, it is clear that the [SSS] pocket receives a metal ion. To support the practical use of this design, **2a**−**3a** were studied by UV−vis and fluorescence spectroscopy; **2a** was the most fluorescent by roughly a factor of 10 (Φ_F = 0.27 ± 0.013 (**2a**), 0.024 ± 0.0016; (**2b**), 0.0034 ± 0.00047 (**3a**)). Importantly, at presaturative low [Cu^{2+}] with **3a** (<3 × 10^{-5} M), an increase (off−on; 6-fold) was observed, whereas for **2a**, on−off signaling was observed. At low mercuric ion concentration ([Hg^{2+}] < 3 × 10^{-5} M), **2b** allowed for a 3-fold (off−on) response, and for **2a** it decreased (on−off). For (Hg^{2+})·**2a**, the association constant (K_a) was determined to be 3120 ± 307 M^{-1}. Detailed multinuclear NMR spectra were acquired (Supporting Information) showing various peaks that correspond to all expected protons and carbons. Some NMR methods utilized herein included ^{1}H−^{1}H COSY, ^{1}H−^{1}H NOESY, ^{1}H−^{13}C HMQC, and ^{1}H−^{13}C HMBC spectroscopy; this allowed for a thorough NMR spectral characterization of these new BODIPY species. We hope that this report serves as an impetus for pursuing different metal ion detection studies where subtle sterics might impart discrete and differing optical effects. We hope that such advances in sensing can later impact the field of molecular neurodegeneration research.

ASSOCIATED CONTENT

Supporting Information. X-ray crystallographic data for compounds **2a** and **3a** (CIF). Photophysical data of compounds **1a**, **2a**, **2b**, and **3a**. ^{1}H, ^{13}C, and ^{11}B NMR spectra and ^{1}H-^{1}H COSY, ^{1}H-^{1}H NOESY, ^{1}H-^{13}C HMQC, and ^{1}H-^{13}C HMBC NMR spectra. High-resolution MALDI-TOF mass spectra and elemental analysis data. Energy diagrams and selected molecular orbital diagrams. This material is available free of charge via the Internet at http://pubs.acs.org.

AUTHOR INFORMATION

Corresponding Author
*E-mail: dchurchill@kaist.ac.kr.

ACKNOWLEDGMENT

D.G.C. acknowledges research support from NRF (Grant No. N01090203) and from the High Risk High Return Project (HRHRP) at KAIST (Grant No. N10100016). Mr. Hack Soo Shin is again gratefully acknowledged for his help in acquiring NMR spectroscopic data. MALDI-TOF data were gratefully obtained with the help of the KAIST Research Supporting Team. Teresa Linstead (Cambridge, U.K.) is thanked for her assistance

in efficiently filing structures CCDC 788639 (**3a**) and 788640 (**2a**). W. A. Goddard is thanked for helpful discussions related to prospective solution/calculation work of **2a** and **3a** during his continued stay at KAIST, funded by the World Class University (WCU) Program.

REFERENCES

(1) Brewer, G. J. *Chem. Res. Toxicol.* **2010**, *23*, 319.
(2) Sparks, D. L.; Schreurs, B. G. *Proc. Natl. Acad. Sci. U.S.A.* **2003**, *100*, 11065.
(3) Valko, M.; Morris, H.; Cronin, M. T. D. *Curr. Med. Chem.* **2005**, *12*, 1161.
(4) Bruijn, L. I.; Miller, T. M.; Cleveland, D. W. *Annu. Rev. Neurosci.* **2004**, *27*, 723.
(5) Lin, W. Y.; Long, L. L.; Chen, B. B.; Tan, W.; Gao, W. S. *Chem. Commun.* **2010**, *46*, 1311.
(6) Lan, G. Y.; Huang, C. C.; Chang, H. T. *Chem. Commun.* **2010**, *46*, 1257.
(7) Xu, Z. C.; Xiao, Y.; Qian, X. H.; Cui, J. N.; Cui, D. W. *Org. Lett.* **2005**, *7*, 889.
(8) Wu, Q. Y.; Anslyn, E. V. *J. Am. Chem. Soc.* **2004**, *126*, 14682.
(9) Markesbery, W. R. *Free Radic. Biol. Med.* **1997**, *23*, 134.
(10) Clarkson, T. W. *Environ. Health Perspect.* **2002**, *110*, 11.
(11) Nolan, E. M.; Lippard, S. J. *Chem. Rev.* **2008**, *108*, 3443.
(12) Ulrich, G.; Ziessel, R.; Harriman, A. *Angew. Chem., Int. Ed.* **2008**, *47*, 1184.
(13) Loudet, A.; Burgess, K. *Chem. Rev.* **2007**, *107*, 4891.
(14) Lee, H. Y.; Son, H.; Lim, J. M.; Oh, J.; Kang, D.; Han, W. S.; Jung, J. H. *Analyst* **2010**, *135*, 2022.
(15) Lee, H. Y.; Bae, S. Y.; Jin, J. S.; Jung, J. H. *J. Nanosci. Nanotechnol.* **2010**, *10*, 2416.
(16) Domaille, D. W.; Zeng, L.; Chang, C. J. *J. Am. Chem. Soc.* **2010**, *132*, 1194.
(17) Jiao, L. J.; Li, J. L.; Zhang, S. Z.; Wei, C.; Hao, E. H.; Vicente, M. G. H. *New J. Chem.* **2009**, *33*, 1888.
(18) Choi, S. H.; Pang, K.; Kim, K.; Churchill, D. G. *Inorg. Chem.* **2007**, *46*, 10564.
(19) Miller, E. W.; Zeng, L.; Domaille, D. W.; Chang, C. J. *Nat. Protoc.* **2006**, *1*, 824.
(20) Meallet-Renault, R.; Herault, A.; Vachon, J. J.; Pansu, R. B.; Amigoni-Gerbier, S.; Larpent, C. *Photochem. Photobiol. Sci.* **2006**, *5*, 300.
(21) Jiang, J. L.; Lu, H.; Shen, Z. *Chin. J. Inorg. Chem.* **2010**, *26*, 1105.
(22) Atilgan, S.; Kutuk, I.; Ozdemir, T. *Tetrahedron Lett.* **2010**, *51*, 892.
(23) Fan, J. L.; Guo, K. X.; Peng, X. J.; Du, J. J.; Wang, J. Y.; Sun, S. G.; Li, H. L. *Sens. Actuators, B* **2009**, *142*, 191.
(24) Kim, H. J.; Kim, S. H.; Kim, J. H.; Lee, E. H.; Kim, K. W.; Kim, J. S. *Bull. Korean Chem. Soc.* **2008**, *29*, 1831.
(25) Du, J. J.; Fan, J. L.; Peng, X. J.; Li, H. L.; Wang, J. Y.; Sun, S. G. *J. Fluoresc.* **2008**, *18*, 919.
(26) Yuan, M. J.; Li, Y. L.; Li, J. B.; Li, C. H.; Liu, X. F.; Lv, J.; Xu, J. L.; Liu, H. B.; Wang, S.; Zhu, D. *Org. Lett.* **2007**, *9*, 2313.
(27) Qi, X.; Kim, S. K.; Jun, E. J.; Xu, L.; Kim, S. J.; Yoon, J. *Bull. Korean Chem. Soc.* **2007**, *28*, 2231.
(28) Coskun, A.; Yilmaz, M. D.; Akkaya, E. U. *Org. Lett.* **2007**, *9*, 607.
(29) Wang, J. B.; Qian, X. H. *Org. Lett.* **2006**, *8*, 3721.
(30) Arroyo, I. J.; Hu, R. R.; Merino, G.; Tang, B. Z.; Peña-Cabrera, E. *J. Org. Chem.* **2009**, *74*, 5719.
(31) Choi, S. H.; Kim, K.; Jeon, J.; Meka, B.; Bucella, D.; Pang, K.; Khatua, S.; Lee, J.; Churchill, D. G. *Inorg. Chem.* **2008**, *47*, 11071.
(32) Kee, H. L.; Kirmaier, C.; Yu, L. H.; Thamyongkit, P.; Youngblood, W. J.; Calder, M. E.; Ramos, L.; Noll, B. C.; Bocian, D. F.; Scheidt, W. R.; Birge, R. R.; Lindsey, J. S.; Holten, D. *J. Phys. Chem. B* **2005**, *109*, 20433.
(33) Sun, Z. N.; Liu, F. Q.; Chen, Y.; Tam, P. K. H.; Yang, D. *Org. Lett.* **2008**, *10*, 2171.
(34) Peña-Cabrera, E.; Aguilar-Aguilar, A.; Gonzalez-Dominguez, M.; Lager, E.; Zamudio-Vazquez, R.; Godoy-Vargas, J.; Villanueva-Garcia, F. *Org. Lett.* **2007**, *9*, 3985.
(35) Choi, S. H.; Kim, K.; Lee, J.; Do, Y.; Churchill, D. G. *J. Chem. Crystallogr.* **2007**, *37*, 315.
(36) Demas, J. N. In *Optical Radiation Measurements*; Mielenz, K. D., Ed.; Academic Press: New York, 1982; Vol. 3, pp 195.
(37) Speckbacher, M.; Yu, L. H.; Lindsey, J. S. *Inorg. Chem.* **2003**, *42*, 4322.
(38) Yoshimatsu, M.; Sakai, M.; Moriura, E. *Eur. J. Org. Chem.* **2007**, 498.
(39) Sheldrick, G. M. *SHELXTL, An Integrated System for Solving, Refining and Displaying Crystal Structures from Diffraction Data*; University of Göttingen: Göttingen, 1981.
(40) Frisch, M. J.; Trucks, G. W.; Schlegel, H. B.; Scuseria, G. E.; Robb, M.; Cheeseman, J. R.; Montgomery, J. A.; Vreven, J. A.; Kudin, K. N.; Burant, J. C.; Millam, J. M.; Iyengar, S. S.; Tomasi, J.; Barone, V.; Mennucci, B.; Cossi, M.; Scalmani, G.; Rega, N.; Petersson, G. A.; Nakatsuji, H.; Hada, M.; Ehara, M.; Toyota, K. ; Fukuda, R.; Hasegawa, J.; Ishida, M.; Nakajima, T.; Honda, Y.; Kitao, O.; Nakai, H.; Klene, M.; Li, X.; Knox, J. E.; Hratchian, H. P.; Cross, J. B.; Adamo, C.; Jaramillo, J; Gomperts, R.; Stratmann, R. E.; Yazyev, O.; Austin, A. J.; Cammi, R.; Pomelli, C.; Ochterski, J. W.; Ayala, P. Y.; Morokuma, K.; Voth, G. A.; Salvador, P.; Dannenberg, J. J.; Zakrzewski, V. G.; Dapprich, S.; Daniels, A. D.; Strain, M. C.; Farkas, O.; Malick, D. K.; Rabuck, A. D.; Raghavachari, K.; Foresman, J. B.; Ortiz, J. V.; Cui, Q.; Baboul, A. G. ; Clifford, S. ; Cioslowski, J.; Stefanov, B. B.; Liu, G.; Liashenko, A.; Piskorz, P.; Komaromi, I.; Martin, R. L.; Fox, D. J.; Keith, T.; Al-Laham, M. A.; Peng, C. Y.; Nanayakkara, A.; Challacombe, M.; Gill, P. M. W.; Johnson, B.; Chen, W.; Wong, M. W.; Gonzalez, C.; Pople, J. A. *Gaussian 03*, Revision A. 1; Gaussian, Inc.: Pittsburgh, PA, 2003.
(41) Becke, A. D. *J. Chem. Phys.* **1993**, *98*, 5648.
(42) Lee, C. T.; Yang, W. T.; Parr, R. G. *Phys. Rev. B* **1988**, *37*, 785.
(43) Hay, P. J.; Wadt, W. R. *J. Chem. Phys.* **1985**, *82*, 299.
(44) Petersson, G. A.; Bennett, A.; Tensfeldt, T. G.; Allaham, M. A.; Shirley, W. A.; Mantzaris, J. *J. Chem. Phys.* **1988**, *89*, 2193.
(45) Binkley, J. S.; Pople, J. A.; Hehre, W. J. *J. Am. Chem. Soc.* **1980**, *102*, 939.
(46) Yu, L. H.; Muthukumaran, K.; Sazanovich, I. V.; Kirmaier, C.; Hindin, E.; Diers, J. R.; Boyle, P. D.; Bocian, D. F.; Holten, D.; Lindsey, J. S. *Inorg. Chem.* **2003**, *42*, 6629.
(47) Churchill, D. G. *J. Chem. Educ.* **2006**, *83*, 1798.